PERIODICO di MINERALOGIA
established in 1930

Dipartimento di Scienze della Terra
Sapienza Università di Roma

An International Journal of
Mineralogy, Crystallography, Geochemistry,
Ore Deposits, Petrology, Volcanology
and applied topics on Environment, Archaeometry and Cultural Heritage

Major-trace elements geochemical characterization, geochronology and radiogenic isotopes of Eocene magmatic rocks in Anique, Qaradagh pluton, NW Iran

Shohreh Hassanpour [*,1] and Ghahraman Sohrabi [2]

[1] Department of Geology, Payame Noor University, Iran
[2] Department of Geology, University of Mohaghegh Ardabili, Ardabil, Iran

ARTICLE INFO

Submitted: April 2018
Accepted: June 2018
Available on line: July 2018

* Corresponding author:
hassanpour@pnu.ac.ir

DOI: 10.2451/2018PM789

How to cite this article:
Hassanpour S. and Sohrabi G. (2018)
Period. Mineral. 87, 173-191

ABSTRACT

The Qaradagh batholith straddles the border between Armenia and NW Iran and is a constituent of the Arasbaran Magmatic Belt (AMB). The Qaradagh batholith is composed of several distinct basic to intermediate and felsic intrusions, cross cut by various dykes. $^{40}Ar/^{39}Ar$ biotite step-heating plateau ages of 40.52±0.44 Ma for a granodiorite intrusion indicate that intrusive activity is of early Eocene age. These intrusions are generally biotite, amphibole, magnetite, and titanite-bearing oxidized I-type and can be determined as magnetite series Cordilleran granitoids. They are enriched in LILE, relatively enriched in LREE, depleted in some HFS elements specially Ti, Nb, Ta (TNT) and P, and relatively depleted in HREE. They also have distinctly low Rb/Sr ratios (mainly 0.08-0.525), consistent with derivation from mantle wedge materials and limited contribution from crustal materials. The granitoids have arc-like signatures and the relatively flat HREE patterns (Sm/Yb=1.08-5.29). The restricted range of initial $^{87}Sr/^{86}Sr$ (0.7043 to 0.7050) and positive εNd_i values (+3.1 to +2.5) suggest depleted mantle- derived magmas were the primary source of these granitoids. Based on the chronology results, the Anique granitoids were the earliest bodies intruding the AMB which took place during the early stages of subduction evolution. These magmatic units were emplaced along the ocean-ward portion of the AMB continental arc. The major and trace element, and Sr-Nd isotope geochemistry indicates that these granitoids have mantle- dominated characteristics, which suggests accretion of new continental crust in the Early Cenozoic in this part of the northwestern Iranian Micro-Continent.

Keyword: Qaradagh batholiths; geochemistry; Cordilleran granitoid; continental arc.

INTRODUCTION

Granitic rocks or granitoids are the most abundant rock types in the continental crust (Frost et al., 2001) that display great diversity in their origins, evolution processes and geneses under different tectonic settings (Barbarin, 1999). Various studies provide examples of the importance of source materials in determining the chemical, petrological and isotopic characteristics of granites. There is also a strong link between mineralogical assemblages, petrogenetic types, source regions and geodynamic environments (Anthony, 2005; Barbarin, 1999; Wu et al., 2003).

The complex is part of the AMB magmatic arc, which is located in the northwestern Iranian micro-plate and extends northwest into the Lesser Caucasus (Berberian et al., 1981; Hassanpour, 2010; Sohrabi, 2006, 2015). The study area (Qaradagh magmatic belt) is a part of the Arasbaran Magmatic Belt, a metallogenic zone of the eastern Pontide-Lesser Caucasus-Arasbaran-western Alborz chain which itself is located within the Alpine-

Himalayan metallic province. The Qaradagh batholith is situated immediately south of the Aras Border River, and geologically is the Iranian segment of "Ordubad Batholith" of the Lesser Caucasus Zone (Hassanpour, 2010; Hassanpour et al., 2014; Zakeri, 2013; Sohrabi, 2015).

The Arasbaran Magmatic Belt (AMB) is located in the north of Iran, Azerbaijan Province and comprises various Jurassic to Quaternary volcano-plutonic suites. To the north, this belt extends into the Lesser Caucasus region in the south of northern Azerbaijan and the Armenian Republic (Mederer et al., 2013; Sahakyan et al., 2016) (Figure 1).

The Eocene Qaradagh batholith, which is the largest granitoid body in NW Iran, hosts various Cu-Mo-Au bearing porphyry-style and related vein type deposits. We have used major and trace element chemistry and Sr-Nd radio-isotope data of plutons from the inner part of Qaradagh batholith to outline the type, tectonic setting, origin, and oxidation state of the batholith.

GEOLOGICAL SETTING

Regional and Local Geology

The Qaradagh batholith is bounded to the northeast by a largely Cretaceous (rarely Devonian) metamorphosed volcano-sedimentary sequence, which is the oldest outcrop in this area (Figure 1). The AMB is one of the most important Cu-Mo-Au metallogenic belts of NW Iran which essentially formed as a subduction-related magmatic belt (Hassanpour, 2010; Sohrabi, 2006, 2015; Zakeri, 2013; Zakeri and Hassanpour, 2014). The volcano-plutonic suite contains different compositions and rock types with different crystallization ages that correspond with their diverse origins, evolution processes, emplacement levels and tectonic regimes.

The batholith is mainly composed of several complex granitoid intrusions including gabbro, diorite, quartz diorite, quartz monzonite, quartz monzodiorite, granodiorite and granite in addition to some stocks of quartz monzodiorite to quartz diorite and leuco-granite porphyry. It is frequently cross cut by numerous basic to intermediate and, less commonly, acidic dykes that mainly display NW-SE and intermittently N-S or NE-SW trends.

The contact between the Qaradagh batholith and the metamorphic rocks displays amphibolite facies contact metamorphism in the Qoulan area which overprints regional greenschist-facies metamorphism. Jurassic submarine volcanic rocks of intermediate composition with intercalations of marble are exposed north-east of the Qaradagh batholith. Lower and Upper Cretaceous andesite to basaltic andesite submarine volcanic rocks are interlayered with carbonaceous and flyschoid sedimentary sequences occured to the east, south and west of the Qaradagh batholith. There are faulted and/or metasomatized contacts between Cretaceous rocks and the granitoid intrusives. Occasionally skarn type alteration and mineralization formed in carbonaceous contact zones. Eocene magmatism, which is the most intense and widespread volcanic activity in AMB, is mainly found as andesite and intermediate rock in south part of the batholith.

In the study area, this batholith is composed of several intermediate to acidic intrusions (Figure 2), which display a mineralogy and textures that reflect a history of magmatic fractional crystallization in high-level sub-volcanic magma chambers (NICICO, 2007; Sohrabi, 2003; Zakeri, 2013). The studied intrusions are quartz-diorite; quartz-monzodiorite and granodiorite to biotite granite with younger quartz-monzonite stocks (Sohrabi, 2003, 2015) are located between Anique village and the Qarachilar region (Figure 2). Xenoliths of plutonic country rocks and felsic enclaves are common and especially found near the margins and roof of plutons. Mafic micro-granular to porphyric enclaves are typical and in some instances form clusters within the intrusions. Different parts of the study area are frequently cross-cut by various dykes, commonly andesitic-basaltic, andesitic, dacitic to rhyodacitic and occasionally aplitic in composition (NICICO, 2007; Zakeri, 2013; Zakeri and Hassanpour, 2014).

The Qarachilar-Anique intrusive body is the dominant lithology in the Qaradagh batholith (Figure 2) and is mainly a medium- to fine-grained granodiorite to granite and/or quartz-monzodiorite. It generally displays a subhedral - partly euhedral, equigranular to slightly in-equigranular texture. The pluton likely formed from various magmatic pulses, and displays a hornblende-biotite-quartz monzodiorite composition in the sampled zone.

In the southeastern part of the study area a medium to fine grained equigranular quartz diorite to diorite intrusive body with approximately 3×2 km^2 area is exposed. Post magmatic hydrothermal alteration zones occur in some parts of this pluton, especially at their contact zones with granite porphyry intrusion and spatially associated with faulted zones (Figure 2).

The Qarachilar intrusion forms the north-northeastern part of the study area (Figure 2) and is a medium- to fine-grained hornblende-biotite quartz diorite to biotite quartz monzodiorite and biotite granite. This intrusion has an equigranular (mostly amphibole, biotite and plagioclase porphyries) to semi-equigranular texture. In the Qarachilar region, hydrothermal alteration and mineralization zones are present in two sections (Rezaie Aghdam and Sohrabi, 2010; Mokhtari, 2008; NICICO, 2007; Zakeri, 2013).

Anique is a small stock situated between two major faults close to the center of the study area. The stock is

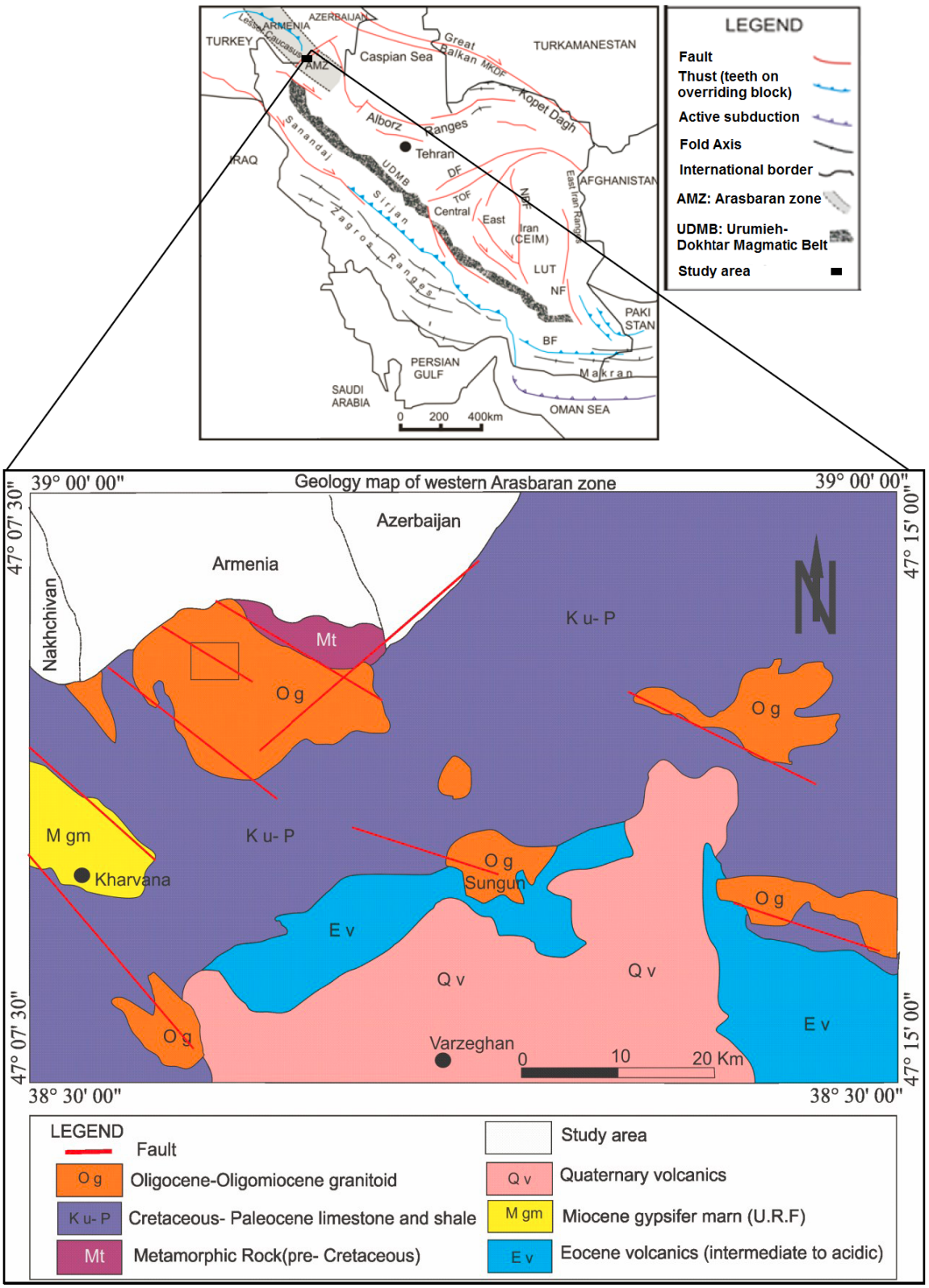

Figure 1. Simplified geological map of the western Arasbaran metallogenic zone in the NW of Iran and its tectonic setting between the NW Iranian microplate and SE Lesser Caucasus region (Sohrabi, 2015).

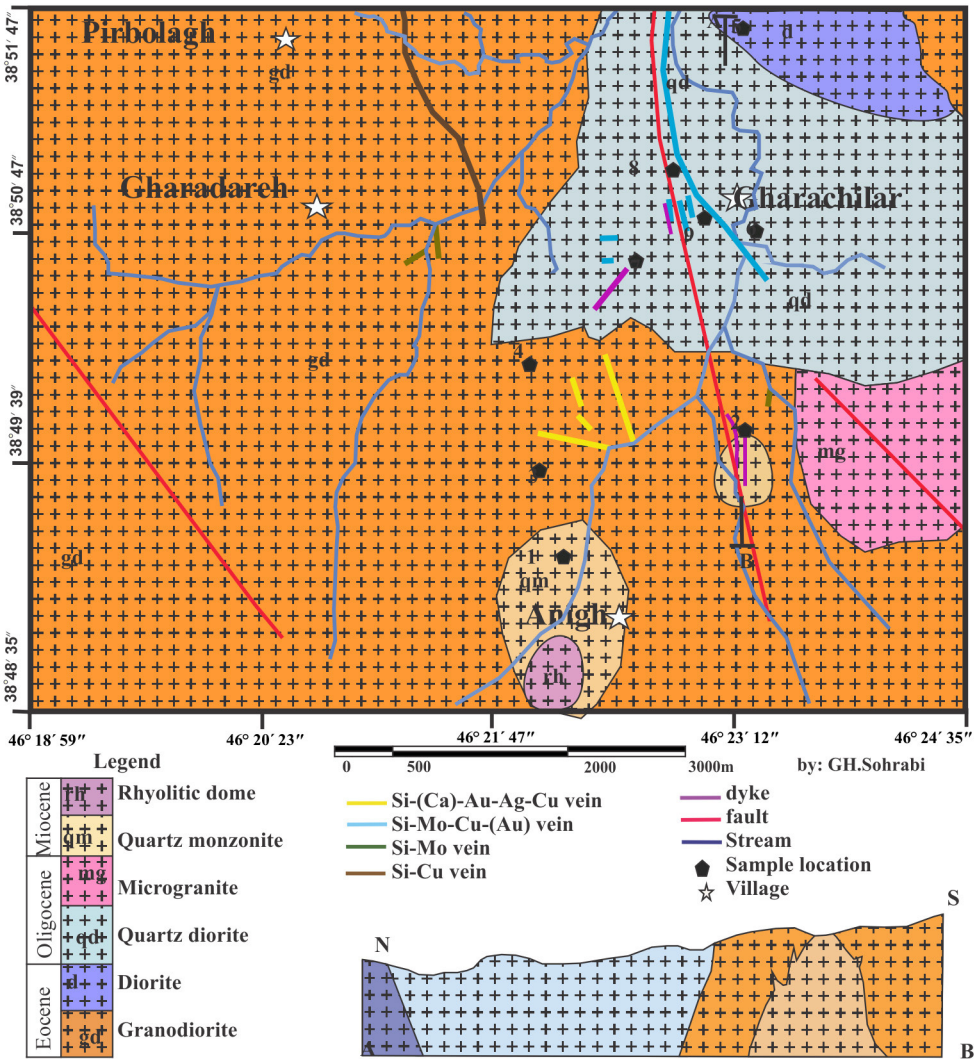

Figure 2. Simplified geological map of the study area with locations of mineralized veins (Sohrabi, 2015).

highly brecciated and altered in the northern and western parts. It is characteristically a medium to fine-grained, hornblende quartz-monzonite to quartz monzodiorite, with equigranular to porphyry-like texture. Andesite, dacite to rhyodacite and porphyritic rhyolite dykes cross-cut this stock, but the genetic relationship of these dykes with mineralization in the Anique district remains unclear due to a lack of field data.

The largest subvolcanic magmatism with porphyritic textures in the study area is a granite porphyry body which has been emplaced into the Anique country rock in the southern part of the Anique body. It is typically formed by pinkish alkali feldspar (up to 1 cm), quartz and a smaller amount of plagioclase porphyry in a fine-grained to aphanitic matrix.

The Qaradagh batholith is dominantly composed of intermediate composition hypabyssal intrusions and various andesitic to rhyolitic dykes, as well as some basic (gabbro) intrusions (Sohrabi, 2003; Mokhtari, 2009; Hassanpour, 2010; Zakeri, 2012).

Petrography

Petrology and petrographic studies show that the composition of intrusive rocks varies from diorite through quartz diorite, monzonite, and granodiorite to granite. All the bodies show similar mineral assemblages and textural characteristics, except for the granite porphyry. Most granitoids typically contain quartz, two feldspars, biotite and amphibole, with accessory magnetite, titanite and apatite. The common textures are medium- to fine-grained, granular to rarely porphyritic. In various samples, monzonitic, microperthitic, felsic, and granophyric

textures are observed (NICICO, 2008; Zakeri, 2013; Zakeri and Hassanpour, 2014; Sohrabi, 2015). Plagioclase commonly forms subhedral to euhedral polysynthetic, twinned crystals and some of them exhibit oscillatory zoning where the rim compositions are relatively more sodic. Alkali feldspar partly displays large microperthitic grains and sometimes alkali feldspar megacrysts are present enclosing euhedral to subhedral plagioclase (Figure 3 a, b), with resorption and/or rarely myrmekite rim textures at the interface between plagioclase and adjacent alkali feldspar grains. Amphibole and biotite are ubiquitous with amount of (10-20%), although considerably variable from one sample to another. Amphibole crystals are generally euhedral or subhedral, indicating early crystallization, and vary in color from brown through greenish brown to pale green. Their color variations are apparently associated with progressively decreasing TiO_2 contents through increasing differentiation of the magma. Hornblende is typically more abundant than biotite in intermediate rocks, except around the potassic alteration and mineralization zones. Biotite and hornblende tend to occur together with euhedral to subhedral magnetite as interstitial clots flanked by felsic minerals (Figure 3 a,b,c and d).

Pyroxene is sometimes present. It is generally associated with dioritic rocks and can be replaced partly or completely by amphibole, which indicates the instability of this mineral during magma evolution during ascent through the crust. Primary magnetite and titanite is abundant in the Anique granitoids; pyrrhotite and ilmenite are commonly absent, whereas pyrite can be present in all stages of mineralizations. Apatite and titanite formed in the early stages of magma crystallization and are typically found as inclusions in plagioclase and amphibole.

ANALYTICAL METHODS

Geochronology

$^{40}Ar/^{39}Ar$ dating

One sample SH440 of primary biotite from the Anique area (granodiorite) was collected from the unmineralized part of the stock for $^{40}Ar/^{39}Ar$ dating (Figure 4). The dated biotite was from primary phenocrysts; $^{40}Ar/^{39}Ar$ dating of these minerals therefore provides constraints on the timing of intrusions of the Anique stock. The sample was crushed, repeatedly sieved to obtain mineral grains as uniform as possible in size, washed in distilled water in an ultrasound bath for half an hour, and dried. Then fine grains were handpicked under a binocular microscope. Extreme care was taken to ensure high purity (>99%) concentrates. Mineral separates were wrapped in aluminum foil and stacked in an irradiation capsule with similar-aged samples and neutron flux monitors (Fish Canyon Tuff sanidine (FCs):28.02 Ma; Renne, et al. 1998).

The samples were irradiated at the McMaster Nuclear Reactor in Hamilton, Ontario, for 43 MWH, with a neutron flux of approximately 6 x 10^{13} neutrons/cm^2/s. Analyses (n=30) of 6 neutron flux monitor positions produced errors of <0.5% of the J value.

The samples were analyzed at the Noble Gas Laboratory, Pacific Centre for Isotopic and Geochemical Research, University of British Columbia, Vancouver, BC, Canada. The mineral separates were step-heated at incrementally higher powers in the defocused beam of a 10 W CO_2 laser (New Wave Research MIR10) until fused. The gas evolved from each step was analyzed by a VG5400 mass spectrometer equipped with an ion-counting electron multiplier. All measurements were corrected for total system blank, mass spectrometer sensitivity, mass discrimination, radioactive decay during and subsequent to irradiation, as well as interfering Ar from atmospheric contamination and the irradiation of Ca, Cl and K isotope production ratios: $(^{40}Ar/^{39}Ar)_K$=0.0302±0.00006, $(^{37}Ar/^{39}Ar)_{Ca}$=1416.4±0.5, $(^{36}Ar/^{39}Ar)_{Ca}$=0.3952±0.0004, Ca/K=1.83±0.01($^{37}Ar_{Ca}/^{39}Ar_K$). The analytical data are shown in Table 1.

ICP Ms-Geochemistry analysis

Approximately all rocks in the study area were subjected to moderate to intense alteration, especially within and proximal to the mineralized zones (Anique, Qarachilar and Zarlidareh regions). Unfortunately, no drill core is available from these areas, and outcrops of fresh igneous rock are only found in the outermost parts of the intrusion. Isotopic studies were carried out on 4 samples submitted for whole-rock analyses of igneous rocks. These samples were analyzed for major elements by inductively coupled plasma-atomic emission spectroscopy (ICP-AES), whereas trace elements were determined using an inductively coupled plasma-mass spectrometer (ICP-MS) at the Amdel laboratory, Australia. The detection limits are 0.01% for all major element oxides and 0.5-1 ppm for rare earth elements. Although some samples are fairly altered, most of them show only minor loss on ignition (LOI≤2 wt%). The representative major and trace element compositions of the Anique - Qarachilar rocks are presented in Table 2.

Sr and Nd isotopes

Four whole-rock samples of the granitoid plutons from the study area have been selected for $^{87}Sr/^{86}Sr$ and $^{143}Nd/^{144}Nd$ isotope analysis carried out at the Pacific Centre for Isotopic and Geochemical Research (PCIGR) at the University of British Columbia in Vancouver, Canada. We have normalized the measured isotopic ratios of the USGS reference materials to SRM 987 $^{87}Sr/^{86}Sr$= 0.710248 relative to the barrel average. For each barrel of 21 filaments, 4 or 5 positions were occupied by a reference

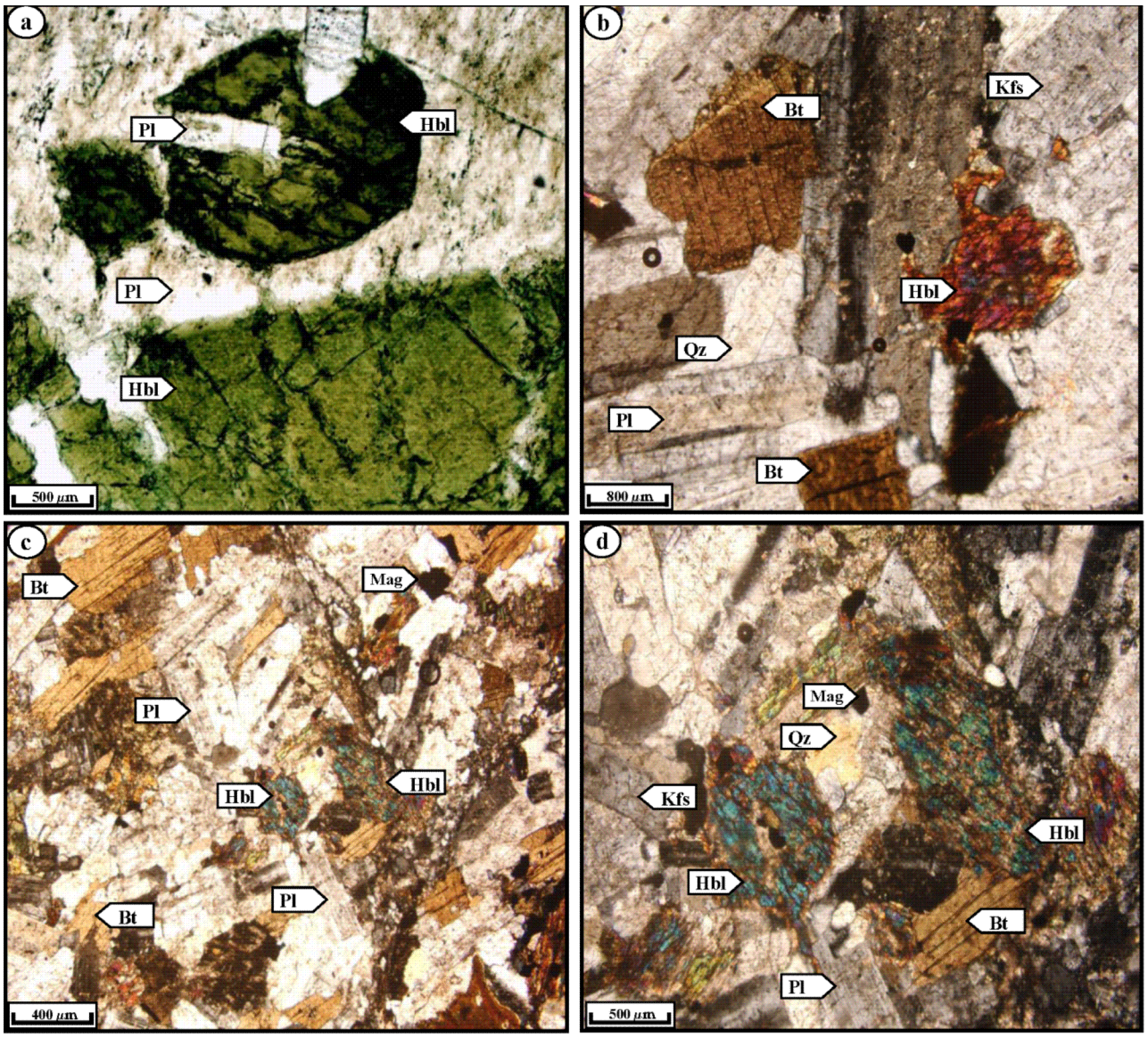

Figure 3. Photomicrographs showing the common mineral assemblages of the studied intrusions of the Qaradagh batholith. (a) Diorite from Anique quartz diorite, hornblende (Hbl) and plagioclase (Pl) found with euhedral to subhedral crystals. (b) Anique quartz monzonite with large grain of plagioclase (Pl), alkali feldspar (Kfs) and biotite (Bt). (c), (d) Quartz diorite (to diorite) from Anique pluton containing large zoned plagioclase (Pl) with hornblende (Hbl), quartz (Qz), and magnetite.

material (SRM 987 for Sr and La Jolla or Rennes for Nd). The average of these 4 or 5 analyses corresponds to the barrel average. The normalization procedure has been applied to the Nd isotopic ratios for the La Jolla and Rennes reference materials, with a normalization value of $^{143}Nd/^{144}Nd$=0.511858 (Lugmair et al., 1983) and 0.511973 (Chauvel and Blichert-Toft, 2001), respectively.

Sr and Nd isotopic compositions were measured in static mode with relay matrix rotation (the ‘‘virtual amplifier’’ of Finnigan) on a single Ta and double Re-Ta filament, respectively. The data were corrected for mass fractionation by normalizing to $^{86}Sr/^{88}Sr$=0.1194 and $^{146}Nd/^{144}Nd$=0.7219, using an exponential law. Replicate analyses of the La Jolla Nd reference material on the Triton TIMS gave 0.511850±15 and then 0.511853±12 (n=118) after one of the Faraday cups was changed. We also analyzed the Rennes Nd reference material (Chauvel and Blichert-Toft, 2001) and obtained $^{143}Nd/^{144}Nd$= 0.511970±10 (n=10). Replicate analyses of the Sr reference material SRM 987 yielded $^{87}Sr/^{86}Sr$ values of 0.710256±16 (n=145) and then 0.710252±13 (n=88) after one of the Faraday cups was changed. Usually, a single

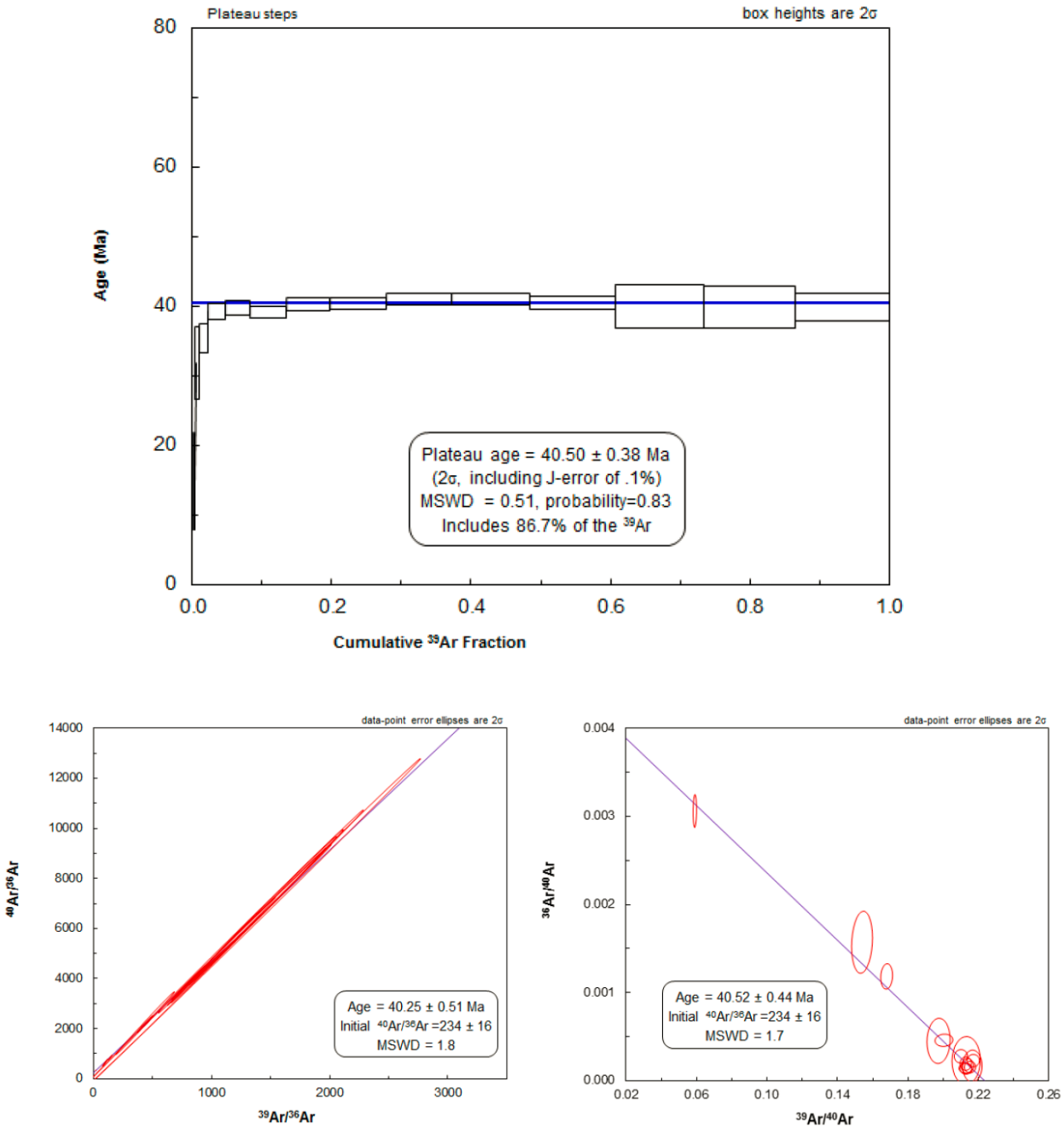

Figure 4. $^{40}Ar/^{39}Ar$ step-heating diagram with plateau age. B. normal and C. inverse isotope correlation diagram for biotite from sample SH440.

analysis consisted of a minimum of ratios (9 blocks of 15 cycles) to allow for a full rotation of the virtual amplifier. The number of blocks must match the number of collectors used, i.e., 5 for Sr and 8 for Nd. Four or five standards are loaded per 21 sample barrel. Nd isotopic compositions were also measured on the Nu Plasma, by static multicollection with Faraday cups on aliquots of the same sample solutions used for TIMS analyses and on separate dissolutions. Instrument parameters and collector configurations are summarized in Tables 1a, 1b, and 2. Each analysis consisted of 60 ratios (3 blocks of 20 cycles), resulting in a 12-13 minute duration of data collection for each individual analysis. Wash-out time and time for standard replicates after every second sample resulted in an average instrument time of 30 min per sample.

Table 1. Sr and Sm-Nd isotopic data of intrusions from the Qaradagh batholith.

Rock Type	X	Y	$^{87}Sr/^{86}Sr$	$^{143}Nd/^{144}Nd$	$^{147}Sm/^{143}Nd$	$^{145}Nd/^{144}Nd$	εNd	Reference
1-Quartz diorite	619532	4299418	0.704	0.513	0.292	0.348	3.043	Hassanpour 2010 Not published
2-Granodiorite	609080	4304173	0.704	0.513	0.291	0.348	2.692	Hassanpour 2010 Not published
3-Granite Porphyry	610151	4268412	0.704	0.513	0.292	0.348	3.199	This Study
4-Quartz monzodiorite	603498	4300794	0.705	0.513	0.292	0.348	2.555	This Study

Table 2. $^{40}Ar/^{39}Ar$ step heating method data from biotite from granodiorite sample SH440. The sample location is shown in Figure 3.

Laser	Isotope Ratios											
	SH440 biotite			(sample/mineral)								
Power(%)	$^{40}Ar/^{39}Ar$	1σ	$^{37}Ar/^{39}Ar$	1σ	$^{36}Ar/^{39}Ar$	1σ	Ca/K	Cl/K	$\%^{40}Ar$ atm	f ^{39}Ar	$^{40}Ar^*/^{39}ArK$	Age	2σ
2.00 W	27.53	18.17	0.65	0.64	0.041	0.174	1.19		-43.65	0.01	39.570	330.75	± 832.88
2.70 W	16.99	0.11	0.10	0.00	0.052	0.001	0.18		90.49	2.34	1.615	14.76	± 6.99
2.90 W	6.53	0.10	0.10	0.01	0.010	0.001	0.18		46.68	1.69	3.482	31.65	± 5.21
0.20 W	5.99	0.05	0.07	0.00	0.007	0.000	0.13		35.28	4.21	3.875	35.20	± 2.01
3.90 W	5.02	0.05	0.02	0.00	0.002	0.000	0.04		14.05	10.15	4.316	39.15	± 1.15
4.20 W	4.79	0.03	0.04	0.00	0.001	0.000	0.07		8.73	9.10	4.374	39.68	± 0.99
4.50 W	4.64	0.03	0.05	0.00	0.001	0.000	0.09		7.31	10.23	4.300	39.01	± 0.89
4.80 W	4.73	0.03	0.03	0.00	0.001	0.000	0.05		6.30	9.51	4.433	40.21	± 0.93
5.10 W	4.68	0.03	0.03	0.00	0.001	0.000	0.06		5.13	10.95	4.437	40.24	± 0.83
5.40 W	4.73	0.03	0.04	0.00	0.001	0.000	0.07		4.63	11.64	4.510	40.90	± 0.83
5.70 W	4.73	0.03	0.05	0.00	0.001	0.000	0.09		4.76	12.71	4.509	40.89	± 0.81
6.00 W	4.71	0.03	0.06	0.00	0.001	0.000	0.10		5.48	8.28	4.451	40.37	± 1.03
6.30 W	5.10	0.07	0.05	0.00	0.002	0.001	0.09		13.84	2.56	4.393	39.85	± 3.07
6.30 W	4.72	0.07	0.08	0.00	0.001	0.001	0.14		7.30	2.57	4.380	39.73	± 3.06
6.60 W	4.65	0.05	0.09	0.01	0.001	0.000	0.17		5.48	3.90	4.394	39.86	± 2.01
Power(%)	$^{40}Ar/^{39}Ar$	1σ	$^{37}Ar/^{39}Ar$	1σ	$^{36}Ar/^{39}Ar$	1σ	Ca/K	Cl/K	$\%^{40}Ar$ atm	f ^{39}Ar	$^{40}Ar^*/^{39}ArK$	1σ	
Total/ Average	4.917	0.011	0.036	0.00	0.001	0.000				99.85	4.402	0.017	

J=0.0050720±0.0000254 Volume ^{39}ArK=1.824 Integrated Date=39.93±0.31 Ma
Plateau Age=40.50±0.38 Ma (2σ including J-error of 0.3%) MSWD=0.51, probability=0.83 86.7% of the ^{39}Ar, steps 8 through 15
Inverse isochron (correlation age) results. plateau steps: Model 1 Solution (±95%-conf.) on 14 points Age = 40.52±0.44 Ma
40/36 intercept: 234±16 MSWD=1.7. Probability=0.054 (at J=0.005072±0.3% 2σ)

RESULTS

Geochronology

The Qaradagh batholith is composed of several distinct basic to intermediate and felsic intrusions, cross cut by various dykes. One sample SH440 of primary biotite from the Anique area (granodiorite) was collected from the unmineralized part of the stock for $^{40}Ar/^{39}Ar$ dating (Figure 4). The dated biotite was from primary phenocrysts; $^{40}Ar/^{39}Ar$ dating of the biotite mineral therefore provides constraints on the timing of intrusion of the Anique granodiorite stock. Step-heating $^{40}Ar/^{39}Ar$ dating of biotite is presented in Table 2 and yields a plateau date of 40.50±0.38 Ma (MSWD=0.51) that encompasses ca. 83% of the total ^{39}Ar release (Figure 4). Normal age of 40.25±0.51 Ma, inverse isochron space a date of 40.52±0.44 Ma are obtained. Then $^{40}Ar/^{39}Ar$ biotite step-heating plateau age of 40.50±0.38 Ma for a granodiorite intrusion indicates that intrusive activity is of early Eocene age.

Whole Rock Geochemistry

Major and trace elements

The major and trace element compositions (Table 2) of the least altered samples have been analyzed. Whole-rock chemistry is used to classify the samples and to explore the influence of source materials on the melt composition. The Eocene-Miocene plutonic rocks consist mainly of granodiorite and quartz diorite with subordinate diorite, monzonite, and quartz monzonite (Figure 6a, b). These rocks have, 59.4- 72.6 wt% SiO_2 and are characterized by low to medium Al_2O_3 (11.4-14.9 wt%), TiO_2 (0.43-0.99 wt%), low to medium Fe_2O_3 (2.75-7.5 wt%), low MgO (0.94-2.24 wt%), and moderate CaO (2.2-6.8 wt%). All of the rocks have K_2O (1.5-4.5 wt%) and Na_2O (2.3-4.25 wt%). Plots of SiO_2 against major oxides (Harker diagrams) are shown in Figure 7. In general, Al_2O_3, TiO_2, Fe_2O_3, CaO, MgO, MnO, correlate negatively with SiO_2, whereas SiO_2 and K_2O correlate positively. Na_2O and P_2O_5 show no correlation with SiO_2. The plutonic rocks exhibit a wide range of trace element contents (Table 1), with the Ba, Rb, and Sr contents showing the largest variations. The Eocene plutonic rocks in the Qaradagh batholiths (Gharachilar-Anique) show broad geochemical similarities (variations of major and trace element with increasing SiO_2), suggesting that they were derived from a similar magma source.

The sample suite is typically metaluminous (Figure 8a). Based on their ferroan and/or magnesian character (Fe-number), calculated as $FeO_{tot}/ (FeO_{tot}+MgO)$, these granitoids are dominantly magnesian (Cordilleran) and do not show a Fe-enrichment trend (Figure 8b).

This petrochemical character is a sensitive indicator for both the source regions and the differentiation of granitic magmas. It has been demonstrated that the Fe/ (Fe+Mg) ratios of magmas are most strongly affected by their differentiation paths. The magnesian granitoids, which are commonly found as differentiates of wet arc magmas, follow relatively oxidizing differentiation trends where the early crystallization of magnetite inhibits iron enrichment during differentiation (Osborn, 1959; Frost et al., 2001). The crystallization of anhydrous silicate from relatively reduced magmas drives a melt to higher Fe-number ratios such as tholeiitic or mildly alkali ferroan granitoids (Frost and Frost, 1997; Frost et al., 2001). Large variations in the source rock materials (Nabelek et al., 1992) and/or the degree of melting (Holtz and Johannes, 1991; Patino Douce and Harris, 1998) cause the crustal melts to show a wide range in Fe-number. The Qaradagh granitoids show only a small range of Fe* (1.8 to 4.57%, total iron) values that are consistent with subduction-related settings.

These magnesian, metaluminous granitoids tend to be dominantly calcic (Figure 8c) which is typical of the plutonic portions of continental magmatic arcs, for example, in the Mesozoic Cordilleran batholiths of western North America. Granitoids from the Qaradagh batholith cross the sub-parallel alkali-lime trends on the modified alkali-lime index (MALI) diagrams and become more alkaline (Figure 5). This suite generally contains amphibole and biotite as well as magnetite and primary titanite and can therefore be determined as a relatively oxidized magnetite series (Takahashi et al., 1980; Ishihara, 1981).

The REE variations provide insights into magma-forming processes and source regions which are important factors in controlling fundamental characteristics of granites. In the chondrite-normalized (Boynton, 1984) REE plots of these intrusives, the light rare earth elements (LREE) are enriched (La/Yb=13.2, La/Sm=5.08), whereas the heavy rare earth elements (HREE) have relatively flat patterns (Figure 9a). Primitive Mantle normalized plots (Sun and McDonough, 1989), show that LREE and LILE enriched but HFSE and HREE elements are depleted and Ta are depleted in the intrusive rocks of the Qaradagh batholith (Figure 9b). This character is typical of subduction-related calc-alkaline magmas (Luhr, 1992; John, 2001) and indicates metasomatism of the upper mantle by melts and/or fluids derived from subducting oceanic crust and sediments, and the subsequent generation of magma and its evolution within the crust. Ti-Nb-Ta depletion indicates oxidizing, hydrous environments that preferentially stabilize oxide phases that incorporate titanium-group elements (Nb, Ta). It is recognized that the magnesian series reveals a close affinity to relatively hydrous, oxidizing magmas and their subduction-related source regions (Frost and Lindsley, 1991).

Ti-Nb-Ta depletion indicates oxidizing, hydrous

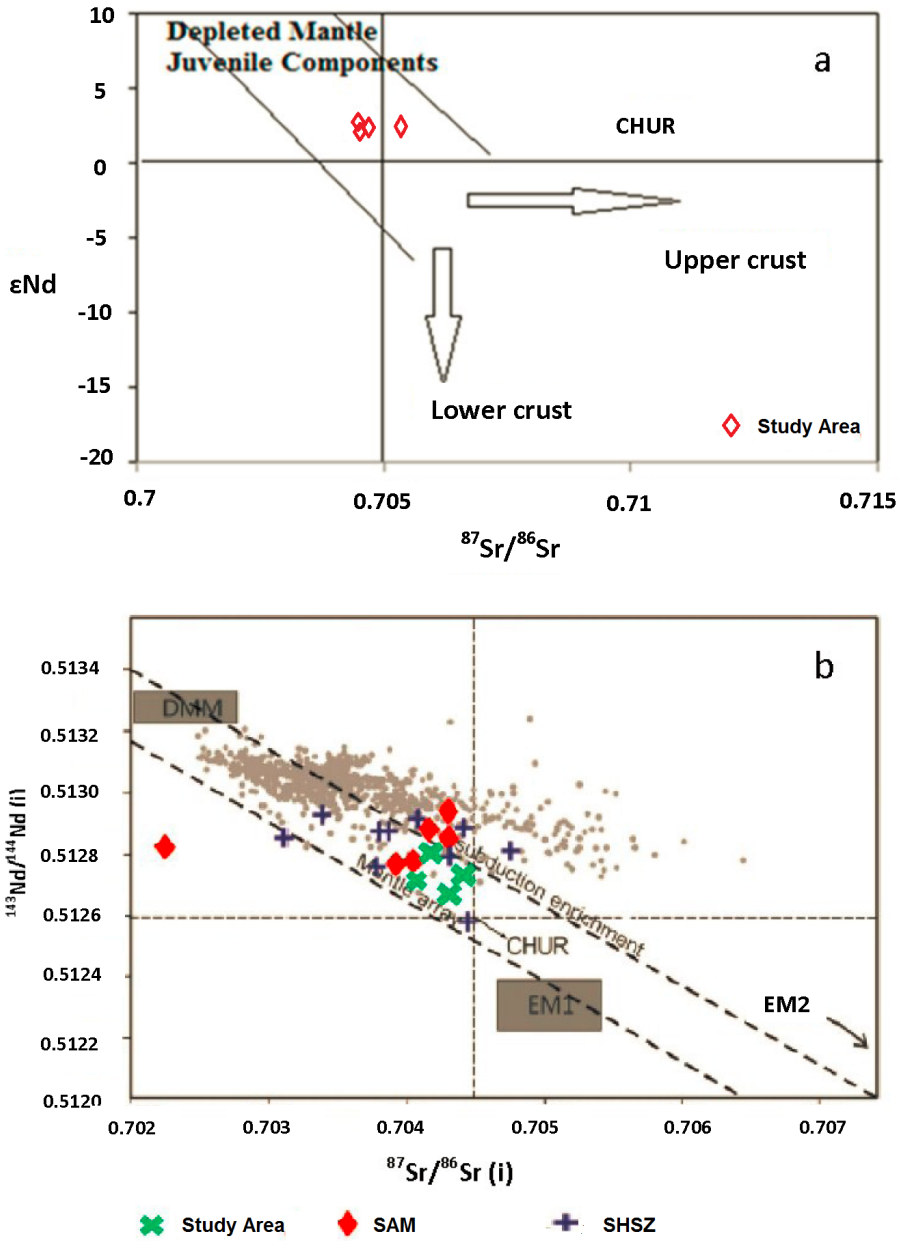

Figure 5. (a) $^{87}Sr/^{86}Sr$ versus εNd diagram (calculated for an age of 40.50±0.38 Ma) for the granitoid plutons of the Qaradagh batholith illustrating a distribution pattern consistent with the mantle array field, indicating a high proportion of depleted mantle-derived material in the generation of these granitoids; CHUR is chondritic unfractionated reservoir. (b) ($^{143}Nd/^{144}Nd$)i vs ($^{87}Sr/^{86}Sr$)i isotope diagrams. The approximate fields for DMM, EM1 and EM2 are from Zindler and Hart (1986). Grey dots: typical volcanic arc data (GEOROC compilation; Sahakayan et al. 2016). Amasia-Sevan-Hakari suture zone (ASHSZ); South Armenian Microplate (SAM). Abbreviations DMM: depleted end member MORB-mantle component; EM, EM1: two "enriched" mantle components (EM and EM I). Red points: Magmatic rocks from SAM; Dark blue: Magmatic rocks from ASHSZ.

environments that preferentially stabilize oxide phases that incorporate titanium-group elements (Nb, Ta). It is recognized that the magnesian series reveals a close affinity to relatively hydrous, oxidizing magmas and their subduction-related source regions (Frost and Lindsley, 1991).

The samples have pronounced arc signatures indicated by high La/Ta (21-145) and Ba/Ta (1147-3179) ratios.

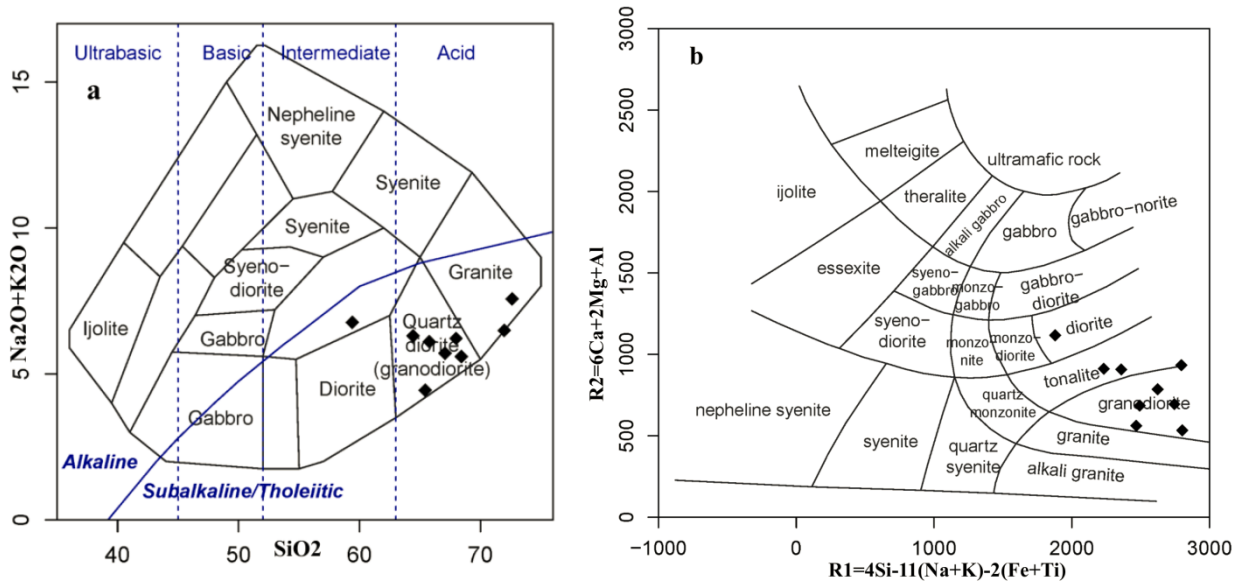

Figure 6. Classification diagrams for the Cenozoic plutonic units of the Qaradagh batholith (Gharachilar-Anique area): (a) Total alkalis vs SiO_2 (Cox et al. 1979) (b) R1-R2 diagram of De La Roche et al. (1980).

Very high La/Ta values reflect differences in solubility of La and Ta in fluids and La/Ta ratios >25 in igneous rocks are generally characterized as arc mantle sources. Furthermore, Ba in arc settings is transported into the mantle wedge by subduction zone fluids, and high Ba/Ta values are typical of magmas which are generated in subduction-related settings (Kay and Mpodozis, 2002). The wide range of Sr concentrations (230.2-723.1 ppm) in these intrusions and low to weakly positive Eu anomaly (Eu/Eu*=0.71-1.16), are compatible with the result of low degree fractional crystallization of hornblende, plagioclase, and accessory phases which can occur during ascent and emplacement of generally oxidized magma (Kay and Mpodozis, 2002).

The low Sm/Yb ratios (1.08-5.29) in these intrusions indicate that their parental magma has been generated under "normal arc" rather than "high pressure" conditions (Kay et al., 1999; Bissig et al., 2003). The low Sr/Y (33.47) and HREE abundances of the Qaradagh granitoids (Table 1) show that residual hornblende, rather than plagioclase, is likely to have controlled the trace element patterns. Because the Sr/Y>40 and Sr/Y<20 boundaries separate adakite from transitional and normal arc fields respectively (Defant and Drummond, 1993), therefore, we propose a normal arc environment during the development of the Qaradagh magmatic system.

We used plots of LREE (La/Sm-Ce/Sm) versus MREE-HREE (Sm/Yb) values (Figure 10 a,b) as a guide to recognize pressure and temperature-sensitive residual mineral assemblages at depth that equilibrated with the parental magmas of the Qaradagh intrusive rocks. These characteristics indicate that the magma equilibrated with dominantly pyroxene, amphibole and garnet-bearing residual assemblages. The presence of garnet in the source rock explains high amount of Sr/Y>40 and Sm/Yb>3 (Kay et al., 1991; Bissig and Tosdal, 2009). These signatures indicate that the magma did not equilibrate with any garnet-bearing mineral residue, whether garnet is in down going slab, the thickened continental crust or in crust mechanically will remove from beneath the arc or fore-arc margin which is recycled into the mantle wedge by fore arc during subduction erosion (Kay et al., 1987, 1991; Hildreth and Moorbath, 1988; Stern, 1991; Kay and Mpodozis, 1999, 2000).

Sr and Nd Isotopic signatures: The Sr-Nd isotopic compositions of Anique intrusives are used to delineate the nature of their source, and to determine the relatively proportion of mantle and crustal components in the generation of these voluminous granitoids. Sr and Nd isotopic data for the four granitoid intrusives of Shah Jahan are given in Table 2. The Sr isotopic data of this suite are shown a restricted range of initial $^{87}Sr/^{86}Sr$ ratios from 0.704 to 0.705, which are relatively low compared with other granitic rocks formed in Phanerozoic orogenic belt, but is quite similar to the Phanerozoic granitoids of the Central Asian Orogenic Belt (Sengor et al., 1993; Jahn et al., 2000; Wu et al., 2003).

For the Sm-Nd isotope data (Table 3), the ε_{Nd} value is

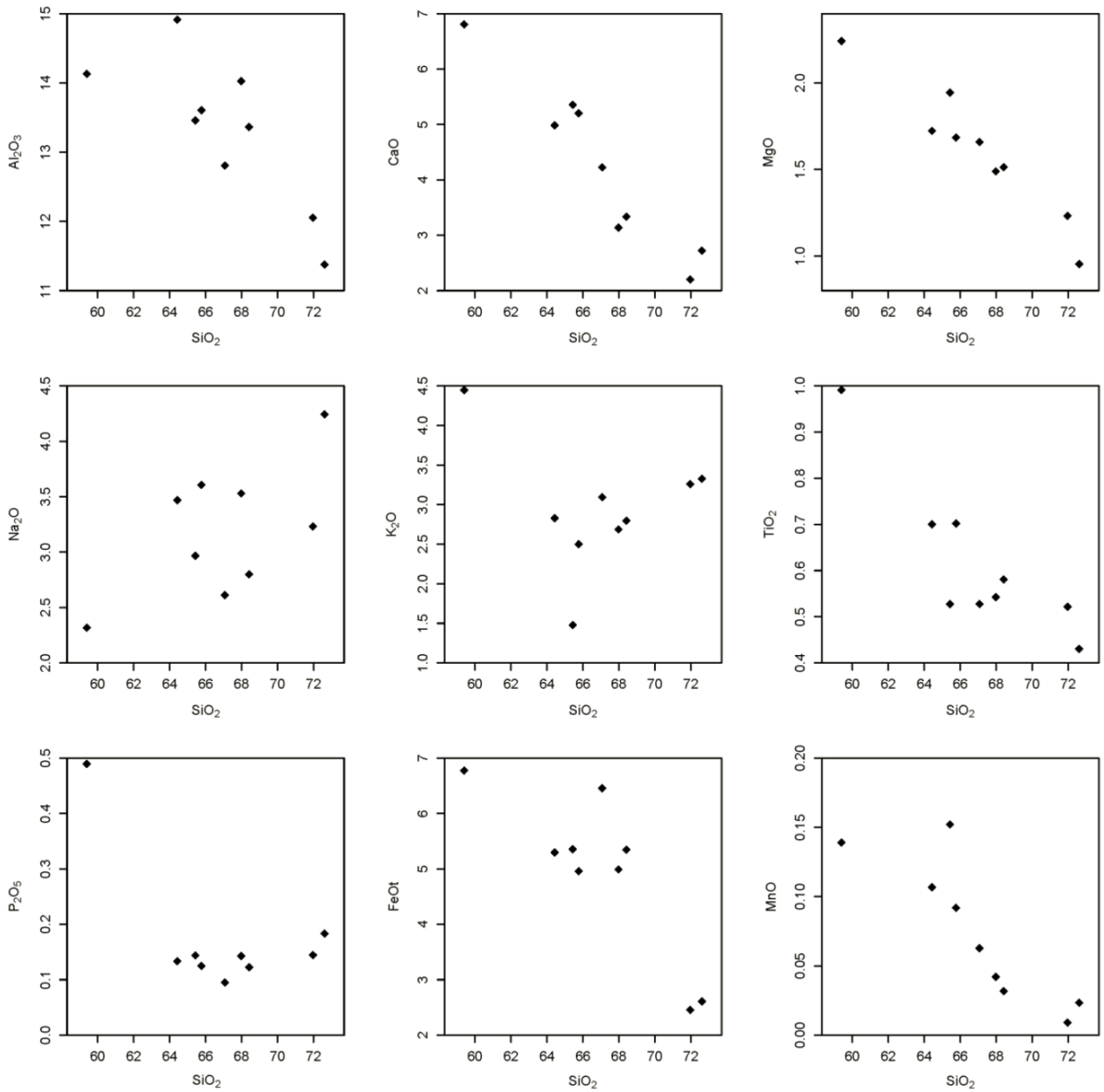

Figure 7. Harker diagrams: SiO_2 plotted against major oxides in the study area.

calculated as:

$\varepsilon_{Nd}= [(^{143}Nd/^{144}Nd)_s/(^{143}Nd/^{144}Nd)_{CHUR}-1] \times 10000$

where s=sample, and $(^{143}Nd/^{144}Nd)_{CHUR}=0.512638$ calculated using CHUR from (Hamilton et al., 1979).

The results show that all samples have positive ε_{Nd} values (+3.1 to+2.5) which demonstrates a high contribution of depleted mantle derived magmas (Figure 5). Based on ε_{Nd} and $^{87}Sr/^{86}Sr$ values of depleted mantle, lower crust and upper crust (ε_{Nd}~+8, -15, -12 and $^{87}Sr/^{86}Sr$~0.703, 0.708, 0.740, respectively; DePaolo et al., 1991), it can be recommended that the Anique magmas were produced probably by melting mantle derived materials (Rapp and Watson, 1995) or older Jurassic-Cretaceous basement arc crust. These granitoids have distinctly low Rb/Sr (≤0.88, mainly 0.1-0.3) with SiO_2 contents ranging from 61 to ~73 weight percent (Table 1) that are based on Blevin and Chappell, 1995 consistent with their derivation from mantle wedge materials and limited interaction with isotopically evolved crustal materials. The present

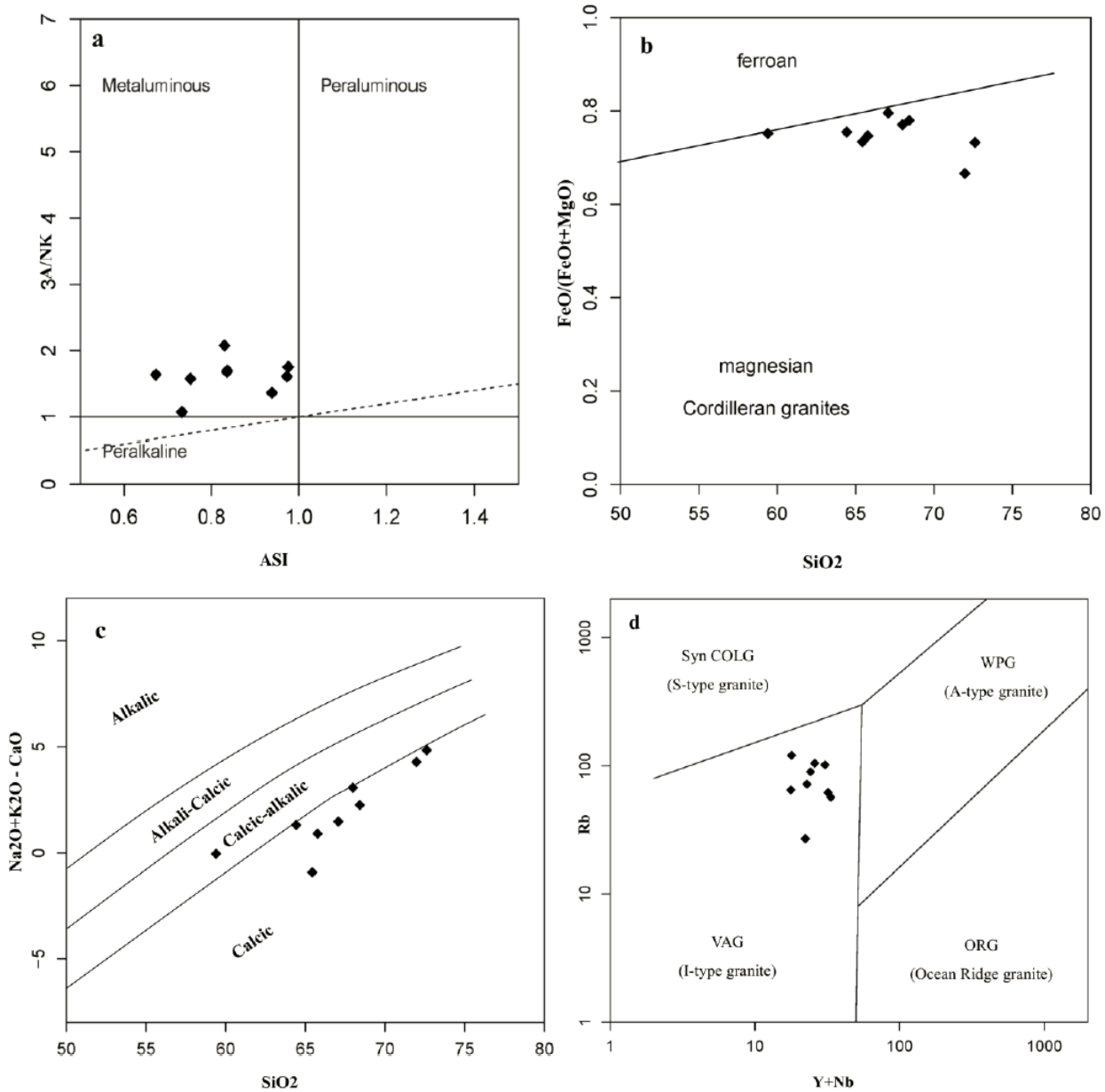

Figure 8. Characteristics of the Qaradagh batholith granitoid samples of (NW-Iran). (a) Metaluminous granitoids in A/NK vs ASI diagram (Maniar and Piccoli 1989). (b) Fe* as FeO^{tot}/ (FeO^{tot}+MgO) vs SiO_2 diagram showing magnesian and Cordilleran granites (Frost et al. 2001). (c) Plot of modified alkali-lime index (MALI) vs. SiO2 showing the mostly calcic and slightly calc-alkalic to alkali-calcic ranges (Frost et al., 2001). (d) Plot of Y+Nb vs Rb diagram showing that the Qaradagh batholith consists of I-type granitoids (Pearce et al., 1984).

geochemical study performed on magmatic rocks of this age from two distinct zones of Armenia, SAM and ASHSZ, suggest their formation occurred in a geodynamic environment in which the source was influenced by a subduction-derived component and contamination by continental crust was absent or very limited.

DISCUSSION

Tectonic setting

This arc formed due to subduction of oceanic crust (a branch of the Meso-Tethys Ocean) beneath a continental margin. The origin of the arc, the initiation of subduction-related magmatism, and the polarity of the subduction zone remain controversial with no general framework

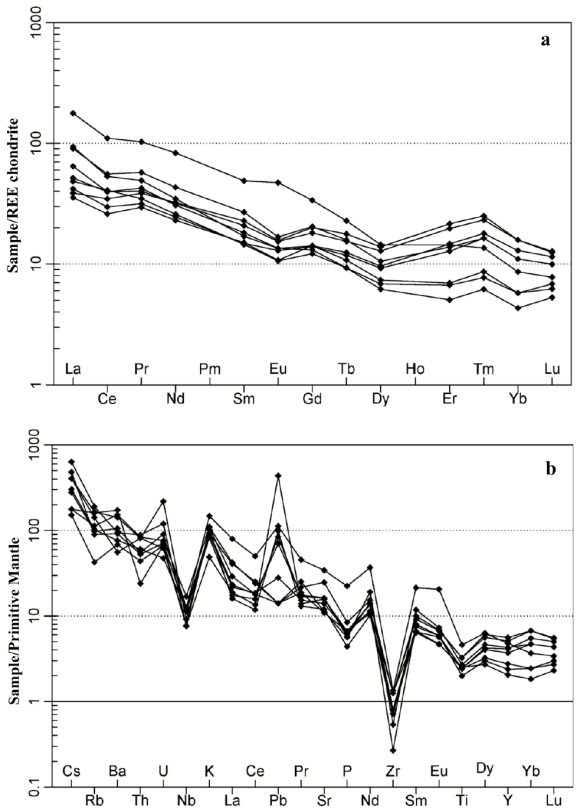

Figure 9. Multi-element diagrams for the Qaradagh granitoid samples. (a) Chondrite-normalized REE diagram, normalization values from Boynton (1984), the pattern shows relative LREE enrichment, whereas the HREE show relatively flat patterns. (b) Primitive mantle- normalized multi element diagram (Sun and McDonough, 1989), all samples are characterized by negative Zr, Nb, Ti and P anomalies, and most of them are enriched in incompatible and large ion lithophile elements (e.g. Rb, Ba, Th, K and Pb).

agreed (e.g. Berberian et al., 1981; Alavi, 1991, 1994, 1996; Calagary, 1997; Nikishin et al., 2001, 2003; Brunet et al., 2003; Azizi and Jahangiri, 2008; Sengor et al., 2008; Hassanpour, 2010; Sohrabi, 2015). However, Hassanpour (2010, 2013 and 2015) proposed a subduction based on magmatic characteristics, age dating and tectonic settings.

The Qaradagh batholith represents the earliest subduction-related magmatic suite in the early stages of AMB development (Hassanpour, 2010). The dioritic intrusion with $^{40}Ar/^{39}Ar$ biotite age (47.63±0.66 Ma and 40.52±0.44 Ma), implying that arc-related intrusive rocks were emplaced during the early Eocene (Hassanpour, 2010). The majority of magmatic activity in the NW AMB (Iranian part) is inferred to have taken place during the Eocene. The Qaradagh batholith was emplaced on the northern-ward portion of the batholithic belt along the north side of the AMB subduction zone.

The intrusions are considered as I-type granitoids (Chappell and White, 1974) which are the most abundant granitoids on Earth and are exposed as plutonic bodies in magmatic arcs (Pearce et al., 1984; Maniar and Picoli, 1989). One of the most important metallogenic features of this Cordilleran type tectono-magmatic setting is the close spatial relationship between arc-related plutonic and volcanic rocks. These intermediate to acidic intrusions are generally accepted as the root zones of formerly active stratovolcanoes (Hattori and Keith, 2001). Sub-volcanic type intrusions emplaced in the shallow crust (<5 km), directly below the polygenetic stratovolcanoes, provide a favorable system in which to form porphyry style Cu-Mo-Au and related high-sulfidation type epithermal Au-Ag deposits (John, 2001). The study area displays widespread Cu-Mo-Au and Au-Ag mineralization. The Qaradagh batholith is flanked by subduction-related

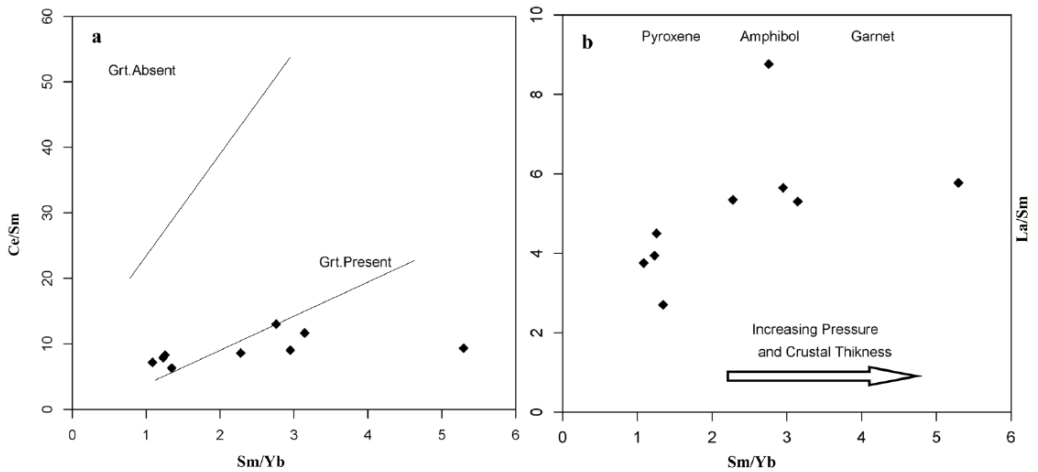

Figure 10. Trace element ratio variation diagrams illustrating the presence of garnet in the source rocks of the Anique granitoids. (a) Ce/Sm vs Sm/Yb (Ileube et al. 1990). (b) La/Sm vs Sm/Yb (Kay and Mpodozis 2001).

Table 3. Major and trace element data for the Anique-Qarachilar granitoid samples.

Sample	SiO_2	Al_2O_3	Fe_2O_3	FeO	CaO	MgO	Na_2O	K_2O	TiO_2	MnO	P_2O_5	LOI
qm-P.Alt	72.61	11.38	2.9	2.61	2.72	0.95	4.24	3.33	0.43	0.02	0.18	1.15
gd-Fr	67.98	14.03	5.55	4.99	3.14	1.49	3.53	2.69	0.54	0.04	0.14	0.81
gd-Fr	64.43	14.91	5.89	5.30	4.98	1.72	3.47	2.83	0.70	0.11	0.13	0.73
gd-Fr	65.77	13.61	5.51	4.96	5.20	1.68	3.61	2.50	0.7	0.09	0.12	1.13
d-Fr	59.40	14.13	7.53	6.78	6.81	2.24	2.32	4.45	0.99	0.14	0.49	1.37
qd-P.Alt	65.43	13.46	5.95	5.36	5.36	1.94	2.97	1.48	0.53	0.15	0.14	2.50
qd-P.Alt	67.07	12.81	7.18	6.46	4.23	1.66	2.61	3.09	0.53	0.06	0.10	0.58
qd-P.Alt	68.42	13.36	5.94	5.35	3.33	1.51	2.80	2.80	0.58	0.03	0.12	1.01
qd-P.Alt	71.97	12.05	2.73	2.46	2.20	1.23	3.23	3.26	0.52	0.01	0.14	2.58
Sample	La	Ce	Nd	Pr	Sm	Eu	Gd	Tb	Dy	Er	Tm	Yb
qm-P.Alt	29	43	20.8	6.00	3.31	0.99	3.39	0.44	2.20	1.40	0.25	1.2
gd-Fr	15	33	15.5	4.24	2.83	0.78	3.15	0.44	1.99	1.05	0.20	0.9
gd-Fr	16	32	19.1	4.90	4.06	1.13	4.69	0.73	4.13	4.13	0.75	3.3
gd-Fr	12	28	19.3	4.70	4.44	1.15	5.19	0.84	4.46	4.52	0.81	3.3
d-Fr	55	89	49.9	12.55	9.53	3.47	8.73	1.08	4.65	3.03	0.44	1.8
qd-P.Alt	13	24	14.7	3.85	2.89	0.95	3.61	0.56	2.97	2.68	0.53	2.3
qd-P.Alt	11	21	13.8	3.60	2.93	0.79	3.67	0.59	3.05	3.08	0.58	2.7
qd-P.Alt	28	45	25.9	6.99	5.24	1.23	5.29	0.75	3.39	2.90	0.53	2.3
qd-P.Alt	20	32	18.4	5.18	3.54	0.99	3.66	0.51	2.37	1.46	0.28	1.2
Sample	Cs	U	Th	Zr	Sb	Sn	V	Co	Ni	Zn	W	Pb
qm-P.Alt	1.4	1.60	7.12	9	0.3	1.2	54	7.9	9	20	4.4	1
gd-Fr	2.4	1.00	5.16	14	0.3	1.2	100	13.9	8	25	1.4	2
gd-Fr	2.2	1.90	4.70	14	0.7	1.7	142	16.1	5	49	1.3	5
gd-Fr	3.8	1.50	4.49	14	1.2	1.5	133	13.8	5	39	0.3	6
d-Fr	1.4	1.40	2.04	15	6.2	1.6	161	13.1	20	51	6.3	8
qd-P.Alt	1.2	1.40	3.74	9	1.9	1.3	117	27.8	10	110	0.3	31
qd-P.Alt	3.2	1.30	6.91	8	0.3	1.1	113	16.7	6	47	3.2	7
qd-P.Alt	3.2	4.60	6.91	6	0.3	1.6	133	19.5	6	49	2.6	1
qd-P.Alt	5.0	2.52	7.56	3	0.3	1.4	120	6.8	6	65	4.1	1
Sample	Lu	Ta	Nb	Y	Ba	Rb	Sr	Cu	Mo	Bi	Hf	Li
qm-P.Alt	0.20	0.58	12.1	10.8	1068	72	523.5	454	13.2	0.3	0.30	7
gd-Fr	0.17	0.40	8.4	9.3	535	65	296.2	232	2.5	0.2	0.30	10
gd-Fr	0.41	0.59	8.9	23.1	739	62	342.7	194	2.1	0.1	1.11	6
gd-Fr	0.40	0.56	8.0	25.4	642	57	340.6	118	1.1	0.1	1.00	7
d-Fr	0.25	0.38	8.9	21.6	1208	102	723.9	11	2.0	0.8	0.76	4
qd-P.Alt	0.32	0.28	5.5	16.8	480	27	333.7	3169	0.6	2.1	0.62	12
qd-P.Alt	0.37	0.34	5.5	18.7	390	90	253.0	2660	4.2	2.5	0.30	7
qd-P.Alt	0.32	0.32	6.5	19.4	995	105	237.0	6667	33.7	1.8	0.30	12
qd-P.Alt	0.22	0.26	5.4	12.5	660	12	230.2	14006	27.8	48.3	0.30	7

Mesozoic-Cenozoic volcanic rocks, and there is no exposure or indirect evidence of a Precambrian basement. Trace element signatures of the Anique granitoids show a moderately low-pressure environment related to partial melting corresponding with source regions under a respectively thickened crust. Ancient Precambrian basement would have a distinctive isotopic geochemical signature which should be picked up by later ascending

magmas. The relatively depleted isotopic compositions of these granitoids indicate their contribution to crustal growth in the AMB in the Mesozoic-Cenozoic. Hence these granitoids are essentially comparable with Mesozoic and younger subduction-related granitoids such as the Canadian Cordillera batholiths (Samson et al., 1991; Silver and Chappell, 1988), and the Andean batholiths of South America (Kay and Rapela, 1990).

Metallogeny

Plutons overlying batholiths in active continental margins provide invaluable information about high-level (<10 km) magma storage reservoirs that are fed by conduits extending into deep-seated mantle magma reservoirs. For Anique there are abundant petrographical and geochemical data from low-pressure crystal fractionation trends that provide strong supporting evidence for the existence of a similar high-level crustal magma reservoir. In regions of thickened continental crust, where magmas must pass through ≥50 km of crust before reaching high-level magma storage reservoirs, magmas often exhibit a strong imprint of continental crustal contamination, which is in contrast to results from the Anique granitoids. For these rocks the Sr-Nd isotopic data and other chemical features indicate a little crustal contamination, and we suggest a discontinuous magma generation and a direct ascent model recommended by Vigneresse (2007), rather than long-lasting lower crustal storage-contamination models like MASH (melt, assimilation, storage, and homogenization; Hildreth and Moorbath, 1988).

It is inferred that the granitoid intrusion of Anique was essentially generated by partial melting of the mantle wedge above subducting oceanic lithosphere (Mokhtari, 2009; Hassanpour, 2010; Sohrabi, 2015). Their chemical signature demonstrates that melting was enhanced by volatile flux from the subducting plate. This is evidenced by LREE-enriched patterns, and high concentrations of large ion lithophile elements (K, Rb, Ba) and Th relative to high field strength elements (Ti, Nb, Ta, Zr, Y). Early crystallization of hydrous minerals (amphibole ± biotite) as well as abundant Fe-Ti oxide minerals in these granitoids, (ilmenite is rare to absent) illustrate that the parental magma was water-rich (>3% to 5% H_2O) and had a relatively high oxygen fugacity (Anthony et al., 2005; John, 2001; Candela, 1997; Burnham, 1979). According to Muller (1971), high magmatic water content is an effective buffer and oxidant, hence the high oxidation state of the Anique magma. Highly oxidized, subduction-related I-type granitoids are amongst those with the highest potential for porphyry style Cu-Mo-Au and associated high-sulfidation Au-Ag mineralization (Zakeri and hassanpour, 2012; Sohrabi, 2015).

CONCLUSIONS

The Qaradagh batholith formed as the earliest subduction-related magmatic suite in the early stage of development of the AMB during the early Eocene. We have interpreted the Qaradagh batholith to have been emplaced on the northern-ward portion of the batholithic belt. (Figure 11). The relatively juvenile isotope compositions of these granitoids as well as their source indicator chemical features indicate a substantial contribution of mantle material in the generation of continental crust in the Anique area. This provides strong evidence for continental crustal growth in the AMB at the Mesozoic-Cenozoic time interval.

Early crystallization of hydrous minerals (amphibole ± biotite) as well as abundant Fe-Ti oxide minerals and rare to absent ilmenite in these granitoids, illustrate that the parental magma was water-rich (>3% to 5% H_2O) and had a relatively high oxygen fugacity. Such a highly oxidized state in these subduction-related I-type granitoids illustrates their potential for porphyry style Cu-Mo-Au and associated high-sulfidation Au-Ag mineralization. We consider such geochemical characteristics to be an important exploration tool in other target granitoids of the Lesser Caucasus - Arasbaran magmatic belt.

ACKNOWLEDGEMENTS

The authors thank British Colombia Ar-Ar dating and radio-isotope centers staffs and Andrew Tunningley for valuable reviews of the manuscript. Also, many thanks to Dr Iain Neill and Dr Martin Timmerman for their so valuable preliminary version of the manuscript editing.

REFERENCES

Alavi M., 1991. Tectonic Map of the Middle East, 1:5000000. Geological survey of Iran.

Alavi M., 1994. Tectonics of the Zagros orogenic belt of Iran: new data and interpretations. Tectonophysics 229, 211-238.

Alavi M., 1996. Tectono-stratigraphic synthesis and structural style of the Alborz Mountain system in Northern Iran. Journal of Geodynamics 21, 1-33.

Anthony E.Y., 2005. Source regions of granites and their links to tectonic environment: examples from the western United States. Lithos 80, 61-74.

Azizi H. and Jahangiri A., 2008. Cretaceous subduction-related volcanism in the northern Sanandaj-Sirjan Zone, Iran. - Journal of Geodynamics 45, 178-190.

Barbarin B., 1999. A review of the relationships between granitoid types, their origins and their geodynamic environments. Lithos 46, 605-626.

Berberian M., Amidi S.M. and Babakhani A., 1981. Discovery of the Qaradagh ophiolite belt: The Southern continuation of the Sevan-Akraophiolite belt in NW Iran (Little Caucasus-Ahar), a preliminary field note. Geological Survey of Iran

551.240 (55) B; 15 pages. Unpublished report.

Bissig T. and Tosdal R.M., 2009. Petrogenetic and metallogenetic relationships in the Eastern Cordillera Occidental of Central Peru. Journal of Geology 117, 499-518.

Blevin P.L., 2004. Metallogeny of granitic rocks, The Ishihara Symposium: Granites and Associated Metallogenesis. Geoscience Australia, 1-4.

Blevin P.L., 2004. Redox and compositional parameters of interpreting the granitoids metallogeny of eastern Australia: Implications for gold-rich ore systems. Resource Geology 54, 241-252.

Blevin P.L. and Chappell B.W., 1992. The role of magma sources, oxidation states, and fractionation in determining the granite metallogeny of eastern Australia, Transactions of the Royal Society of Edinburgh. Earth Sciences 83, 305-316.

Blevin P.L. and Chappell B.W., 1995. Chemistry, origin and evolution of mineralized granites in the Lachlan Fold Belt, Australia: the metallogeny of I- and S-type granites. Economic Geology 90, 1604-1619.

Brunet M.F., Korotaev M., Ershov A.V. and Nikishin A.M., 2003. The South Caspian basin: a review of its evolution from subsidence modelling. Sedimentary Geology 156, 119-148.

Burnham C.W., 1979. Magmas and Hydrothermal Fluids. In Geochemistry of Hydrothermal Ore Deposits, ed., Barnes, H.L., John Wiley & Sons, 71-136.

Calagari A.A., 1997. Geochemical, stable isotope, noble gas, and fluid inclusion studies of mineralization and alteration at Sungun porphyry copper deposit, East Azarbaidjan, Iran: Implication for genesis. Unpublished Ph.D. Thesis, Manchester University, 537 pp.

Candela P., 1997. Shallow, Ore-Related Granites: Textures, Volatiles, and Ore Metals. (For: Special issue on High Level Silicic Magmatism and Related Hydrothermal Systems). Journal of Petrology 38, 1619-1633.

Chappell B. W. and White A.J.R., 1974. Two contrasting granite types. Pacific Geology 8, 173-174.

Chauvel C. and Blichert-Toft J., 2001. A hafnium isotope and trace element perspective on melting of the depleted mantle. Earth and Planetary Science Letters 190, 137-151.

Cox K.G., Bell J.D., Pankhurst R.J., 1979. The interpretation of igneous rocks, George Allen and Unwin, London.

De La Roche H., Leterrier Grandclaude P., Marchal M., 1980. A classification of volcanic and plutonic rock using R1-R2 diagrams and major element analyses, its relationship with current nomenclature. Chemical Geology 29, 183 - 210.

DePaolo D.J., Stolper E.M., Thomas D.M., 1991. Physics and chemistry of mantle plumes. Eos. Transactions of the American Geophysical Union 72.

Frost B.R. and Lindsley D.H., 1991. The occurrence of Fe-Ti oxides in igneous rocks. In: Lindsley D.H. (Ed.), Oxide Minerals: Petrologic and Magnetic Significance. Mineralogical Society of America, Reviews in Mineralogy 25, 433-486.

Frost B.R., Barnes C.G., Collins W.J., Arculus R.J., Ellis D.J., Frot C.D., 2001. A Geochemical classification for granitic rocks. Journal of Petrology 42, 2033-2048.

Hamilton P.J., Evensen N.M., O'Nions R.K., Smith H.S., Erlank A.J., 1979. Sm-Nd dating of Onverwacht Group volcanics, southern Africa. Nature 279, 28-300.

Hassanpour S., 2010. Metallogeney and mineralization of Cu-Au in Arasbaran Zone, NW of Iran, Unpublished Ph.D. Thesis, Shahid Beheshti University, Iran.

Hassanpour S., 2013. The alteration, mineralogy and geochronology (SHRIMP U-Pb and $^{40}Ar/^{39}Ar$) of copper-bearing Anjerd skarn, north of the Shayvar Mountain, NW Iran. International Journal of Earth Sciences 102, 687-699.

Hassanpour S., Alirezaei S. Selby D., Sergeev S., 2015. SHRIMP zircon U-Pb and biotite and hornblende Ar-Ar geochronology of Sungun, Haftcheshmeh, Kighal, and Niaz porphyry Cu-Mo systems: evidence for an early Miocene porphyry-style mineralization in northwest Iran. International Journal of Earth Sciences 104, 45-59.

Hattori K.H. and Keith J.D., 2001. Contribution of mafic melt to porphyry copper mineralization: evidence from Mount Pinatubo, Philippines, and Bingham Canyon, Utah, USA. Mineralium Deposita 36, 799-806.

Hildreth W. and Moorbath S., 1988. Crustal contributions to arc magmatism in the Andes of Central Chile. Contributions to Mineralogy and Petrology 98, 455-489.

Holtz F. and Johannes W., 1991. Genesis of peraluminous granites I. Experimental investigation of melt compositions at 3 and 5 kb and various H2O activities. Journal of Petrology 32, 935-958.

Ileube A., Hirdder W., Mauer R., Kesse G.O., 1990. The early Proterozoic Birimian Supergroup of Ghana and some aspects of its associated gold mineralization. Precambrian Research 46, 139-165.

Ishihara S., 1981. The granitoid series and mineralization. Economic Geology, 75th Anniversary Volume, 458-484.

Jahn B.M., Wu F.Y., Chen B., 2000. Granitoids of the central asian orogenic belt and continental growth in the Phanerozoic. Transactions of the Royal Society of Edinburgh, Earth Sciences 91, 181-193.

Kay S.M. and Mpodozis C., 2000. Chemical signatures from magmas at the southern termination of the Central Andean volcanic zone: The Incappillo/Bonete and surrounding areas. In Congreso Geológico Chileno 9, Actas 1, 626-629. Puerto Varas.

Kay S.M., Mpodozis C., Coira B., 1999. Neogene magmatism, tectonism and mineral deposits of the Central Andes (22°-33°S Latitude). In: Skinner B. (Ed.). Geology and ore deposits of the Central Andes. Society of Economic Geology, Special Publication 7, 27-59.

Kay S., Maksaev V., Mpodozis C., Moscoso R., Nasi C., 1987. Probing the evolving Andean lithosphere; Mid-late Tertiary magmatism in Chile (29- 30.5˚S) over the zone of

subhorizontal subduction. Journal of Geophysical Research 92, 6173- 6189.

Kay S., Mpodozis C., Ramos V.A., Munizaga F., 1991. Magma source variations for mid-Tertiary magmatic rocks associated with a shallowing subduction zone and a thickening crust in the Central Andes (28 - 3˚S). In: R.S. Harmon & C.W. Rapel (Eds.). Andean Magmatism and its Tectonic Setting, Boulder, Colorado , Geological Society of America, Special Papers 265, 113-137.

Kay S.M. and Mpodozis C., 2001. Central Andean ore deposits linked to evolving shallow subduction systems and thickening crust. GSA Today 11, 4-9.

Kay S.M. and Mpodozis C., 2002. Magmatismaz a probe to the Neogene shallowing of the Nazca plate beneath the modern Chilean flat-slab. - Journal of South American Earth Sciences 15, 39-57.

Lugmair G.W., Shimamura T., Lewis R. S., Anders E., 1983. Samarium-146 in the early solar system: Evidence from neodymium in the Allende meteorite. Science 222, 1015-1018.

Luhr J.F., 1992. Slab-derived fluids and partial melting in subduction zones: Insights from two contrasting Mexican volcanoes (Colima and Ceboruco). Journal of Volcanology and Geothermal Research 54, 1-18.

Maniar P.D. and Piccoli P.M., 1989. Tectonic discrimination of granitoids. Geological Society of America, Bulletin 101, 635-643.

Mederer R., Moritz A., Ulianov M., Chiaradia M., 2013. Middle Jurassic to Cenozoic evolution of arc magmatism during Neotethys subduction and arc-continent collision in the Kapan Zone, southern Armenia. Lithos 177, 61-78.

Mokhtari M.A.A., 2009. Petrology, geochemistry and petrogenesis of Qaradagh Batholith (east of Syahrood, Eastern Azerbaijan) and related skarns, with considering mineralization. Unpublished Ph.D. Thesis, Tarbiat Modares University, Iran, 317 pp. (in Persian).

Muller J.E., 1971. Revised geological reconnaissance map of Vancouver Island and Gulf Islands, B. C. Geological Survey of Canada, Open File 61.

Nabelek P.I., Russ-Nabelek C., Denison J.R., 1992. The generation and crystallization conditions of the Proterozoic Harney Peak Leucogranite, Black Hills, South Dakota, USA: petrologic and geochemical constraints. Contributions to Mineralogy and Petrology 110, 173-191.

Nikishin A., Ziegler P.A., Panov D.I., Nazarevich B.P., Brunet M.-F., Stephenson R.A., Bolotov S.N., Korotaev M.V., Tikhomirov P.L., 2001. Mesozoic and Cenozoic evolution of the Scythian Platform - Black Sea- Caucasus domain. In: Ziegler, P.A., Cavazza, W., Robertson, A.H.F., Crasquin-Soleau, S. (Eds.), Peri-Tethys Memoir 6: Peri-Tethyan Rift/ Wrench Basins and Passive Margins. Mémoires du Muséum national d'Histoire naturelle, Paris 186, 295- 346.

Nikishin A.M., Korotaev M.V., Ershov A.V., Brunet M.F., 2003. The Black Sea basin: tectonic history and Neogene-Quaternary rapid subsidence modeling. Sedimentary Geology 156, 149-168.

Patiño Douce A. E. and Harris N., 1998. Experimental constraints on Himalayan anatexis. Journal of Petrology 39, 689-710.

Pearce J.A., Harris N.B.W., Tindle A.G., 1984. Trace element discrimination diagrams for the tectonic interpretation of granitic rocks. Journal of Petrology 25, 956-983.

Rapp R.P. and Watson E.B., 1995. Dehydration melting of metabasalt at 8-32 kbar: Implications for continental growth and crust-mantle recycling. Journal of Petrology 36, 891-931.

Renne P.R.C., Swisher C.C. III, Deino A.L., Karner D.B., Owens T., DePaolo D.J., 1998. Intercalibration of standards, absolute ages and uncertainties in $^{40}Ar/^{39}Ar$ dating. Chemical Geology 145, 117-152.

Rezai-Aghdam M. and Sohrabi Gh., 2010. Geochemistry of Alteration and its Relation to the Minralization of Cu-Mo in the Qarachilar-Qaredareh area (NW Iran). Journal of Science of the Islamic Azad University, Tehran, Iran 20 (77), 129-150 (in Persian).

Sahakayan D. Bosch M., Sosson A., Avagyan GH., Galoyan Y., Rolland O., Bruguier ZH., Stepanyan B., Galland B., Vardayan S., 2016. Geochemistry of the Eocene magmatic rocks from the Lesser Caucasus area (Armenia): evidence of a subduction geodynamic environment. Geological Society, London, Special Publications 428, http://doi.org/10.1144/SP428.12.

Sengor A.M.C., Ozaran M.S., Keskin M., Sakinc M., Ozbakir A.D., Kayan I., 2008. Eastern Turkish high plateau as a small Turkic-type orogen: Implications for post-collisional crust-forming processes in Turkic-type orogens. Earth-Science Reviews 90, 1-48.

Sengor A.M.C., Ozaran M.S., Keskin M., Sakinc M., Ozbakir A.D., Kayan I., 2008. Eastern Turkish high plateau as a small Turkic-type orogen: Implications for post-collisional crust-forming processes in Turkic-type orogens. Earth-Science Reviews 90, 1-48.

Sohrabi Gh., 2003. The study of mineralization Cu-Mo-Fe in Qulan granite, East Azarbaijan. Unpublished M.Sc. Thesis, Tabriz University, Iran, 148 pp. (in Persian).

Sohrabi Gh., 2006. The zonation of Cu-Au and Cu-Mo in metalogenic zone of NW Iran. 25th Symposium of Geosciences, Geological Survey of Iran, Tehran, Iran.

Sohrabi, Gh., 2015. Study of metallogeny and geochemistry of molybdenum deposits in Gharadagh-Sivardagh belt, East-Azarbaidjan, NW Iran. Unpublished Ph.D. Thesis, University of Tabriz, Tabriz, Iran, 609 pp. (in Persian).

Sohrabi Gh., Hosseinzadeh M.R., Calagari A.A., Hadjalilu B., 2015. Study of Mo mineralization in the Gharehdagh (Ordobad)-Shivardagh strip with emphasis on alteration, petrology, and geochemistry of host intrusive bodies (northwest of Iran). Earth Sciences, V., 24(95), 243-258 (in Persian).

Stern C.R., 1991. Role of subduction erosion in the generation of the Andean magmas. Geology 19, 78-81.

Sun S.S. and McDonough W.F., 1989. Chemical and isotopic systematics of oceanic basalts: Implications for mantle composition aand processes. In: Saunders A.D. and Norry M.J. (Eds.), Magmatism in the ocean basins. Geological Society, London, Special Publications 42, 313-345.

Takahashi M., Aramaki S., Ishihara S., 1980. Magnetite-series/ ilmenite-series vs. I-type/S-type granitoids. In Ishihara S. and Takenouchi S. (Eds.), Granitic magmatism and related mineralization Mining. Geology, Special Issue 8, l3-28.

Vigneresse J.L., 2007. the role of discontinuous magma inputs in felsic magma and ore generation. Ore Geology Reviews 30, 181-216.

Wu F.Y., Jahn B.M., Wilde S.A., Lo C.H., Yui T.F., Lin Q., Ge W.C., Sun D.Y., 2003. Highly fractionated I-type granites in NE China (II): isotopic geochemistry and implications for crustal growth in the Phanerozoic. Lithos 67, 191-204.

Zakeri L., 2013. Geological, mineralization, alteration, geochemistry and genesis studies of Garachilar ore deposit - Shah Jahan granitoid batholith (Northwestern Iran), Unpublished Ph.D. Thesis, Tabriz University, Tabriz, Iran (in Persian).

Zakeri L. and Hassanpour S., 2014. Tectonic setting, source region and oxidation state controls on metallogenic characteristics of Cu-Mo-Au mineralized I-type granitoids from the Shah Jahan Batholith, NW Iran. 32nd National & the 1st International Geosciences.

Zindler A. and Hart S., 1986. Chemical Geodynamics. Annual Reviews of Earth and Planetary Sciences 14, 493-571.